Contribution of the electromagnetic dipole operator $\mathcal{O}_7$ to the $\bar{B}_s \to \mu^+\mu^-$ decay amplitude

Thorsten Feldmann[*], Nico Gubernari[†], Tobias Huber[‡] and Nicolas Seitz[§]

Theoretische Physik 1, Center for Particle Physics Siegen (CPPS), Universität Siegen,
Walter-Flex-Straße 3, D-57068 Siegen, Germany

We construct a factorization theorem that allows one to systematically include QCD corrections to the contribution of the electromagnetic dipole operator in the effective weak Hamiltonian to the $\bar{B}_s \to \mu^+\mu^-$ decay amplitude. We first rederive the known result for the leading-order QED box diagram, which features a double-logarithmic enhancement associated with the different rapidities of the light quark in the $\bar{B}_s$ meson and the energetic muons in the final state. We provide a detailed analysis of the cancellation of the related endpoint divergences appearing in individual momentum regions, and show how the rapidity logarithms can be isolated by suitable subtractions applied to the corresponding bare factorization theorem. This allows us to include in a straightforward manner the QCD corrections arising from the renormalization-group running of the hard matching coefficient of the electromagnetic dipole operator in soft-collinear effective theory, the hard-collinear scattering kernel, and the B_s-meson distribution amplitude. Focusing on the contribution from the double endpoint logarithms, we derive a compact formula that resums the leading-logarithmic QCD corrections.

I. INTRODUCTION

The rare decay $\bar{B}_s \to \mu^+\mu^-$ mediated by flavor-changing neutral current $b \to s$ transitions represents one of the golden channels to test the flavor sector of the Standard Model (SM). Precision measurements of its decay rate are performed at current flavor experiments [1–12]. Precise theoretical predictions include higher-order QCD and electroweak corrections (see e.g. Refs. [13–16], for reviews see e.g. Refs. [17,18] and references therein). Comparing experimental precision measurements and theoretical predictions thus allows us to search for indirect effects of physics beyond the SM. As it has been pointed out in Refs. [19,20], at the level of the intended precision, theoretical calculations also have to take into account corrections from nonlocal QED effects. In particular, the exchange of an additional photon between the light degrees of freedom in the $\bar{B}_s$-meson and the final-state muons leads to a power enhancement compared to the leading

contribution from the local semileptonic operator $\mathcal{O}_{10}$. Besides the phenomenological importance, these effects are of particular theoretical relevance for two reasons. First, QED corrections to exclusive decays of heavy quarks at large recoil are conceptually interesting, and the corresponding generalization of the QCD factorization approach is nontrivial [21–24]. Second, the contribution of the electromagnetic dipole operator $\mathcal{O}_7$ features a double-logarithmic enhancement that results from endpoint configurations of the light-cone momentum fractions of the intermediate muon propagator with respect to the external muons. Analyzing the relevant QED box diagram with the method of momentum regions then leads to endpoint-divergent convolution integrals, which makes the formulation of factorization theorems and the renormalization-group improvement for this contribution difficult and nonstandard [25]. The systematic understanding of endpoint logarithms in the context of factorization theorems and effective-field-theory methods is currently a very active field of research. While the analysis of endpoint dynamics and rapidity logarithms for nonperturbative setups, like exclusive charmless b-quark decays [26], is notoriously difficult [27], progress has recently been made for a number of perturbative examples, including bottom-induced $h \to \gamma\gamma$ decay [30,31], off-diagonal gluon thrust [32], or muon-electron backward scattering [33]. In this context, the $\mathcal{O}_7$ contribution to the $\bar{B}_s \to \mu^+\mu^-$ decay amplitude offers another example to study rapidity logarithms in hard exclusive transitions. In this case the origin of the endpoint

[*]thorsten.feldmann@uni-siegen.de
[†]nicogubernari@gmail.com
[‡]huber@physik.uni-siegen.de
[§]nicolas.seitz@uni-siegen.de

double logarithms resides on the muon side and can thus be understood in QED perturbation theory, while the dynamics of the strange quark is embedded in the exclusive hadronic $B \rightarrow$ vacuum transition.

The aim of this work is to provide a QCD factorization theorem for the $\mathcal{O}_7$ contribution to the $\bar{B}_s \rightarrow \mu^+\mu^-$ decay amplitude. To this end, in the following Sec. II, we first rederive the result from Ref. [19] by adding up the relevant momentum regions [34,35] of the QED box diagram. Depending on the choice for the additional regulator that is needed to render the convolution integrals finite, we find different relevant momentum regions. In particular, we show that the double-logarithmic term in the final result can be isolated from a certain momentum configuration, where the photon propagators become eikonal and the intermediate muon propagator goes on shell (see e.g. Ref. [36] and references therein). The results from the analysis of the leading QED box diagram can be generalized to obtain a bare factorization theorem that takes into account additional QCD corrections, depending on the applied regulators. By means of suitable subtractions on the basis of refactorization conditions, we construct a factorization theorem with endpoint-convergent convolutions where the additional analytic regulator can be dropped and the $1/\epsilon$ divergences from dimensional regularization are manifest.

On the basis of this result, it is a rather straightforward task to implement the leading-logarithmic QCD corrections to the $b \rightarrow s\gamma$ vertex, the jet function describing the exchange of a hard-collinear strange quark and the light-cone distribution amplitude (LCDA) of the B_s-meson. This is worked out in detail in Sec. III. On the basis of an explicit and systematic parametrization for the LCDA we also provide a relatively compact formula that resums the leading-logarithmic QCD effects in renormalization-group (RG) improved perturbation theory. A brief numerical analysis shows that the effect of the leading-logarithmic QCD corrections can be of the order of 10%–30% relative to the $\mathcal{O}_7$ contribution at fixed-order $\mathcal{O}(\alpha_s^0)$, depending on the shape of the B_s-meson LCDA. It should, however, be noted that the overall effect of the electromagnetic dipole operator is small because of the associated small Wilson coefficient C_7, such that our result only has a marginal phenomenological impact on the $\bar{B}_s \rightarrow \mu^+\mu^-$ decay rate. We conclude this paper with a short summary. A detailed description of the subtractions that are required to get rid of endpoint-divergent convolution integrals in the bare factorization theorem is provided in the Appendix.

II. THE LEADING-ORDER QED BOX DIAGRAM

Our starting point is the nonlocal matrix element

$$\langle 0 | \int d^4x \, T\{j_{\text{em}}^\mu(x), \mathcal{H}_{\text{eff}}(0)\} | \bar{B}_s \rangle \tag{1}$$
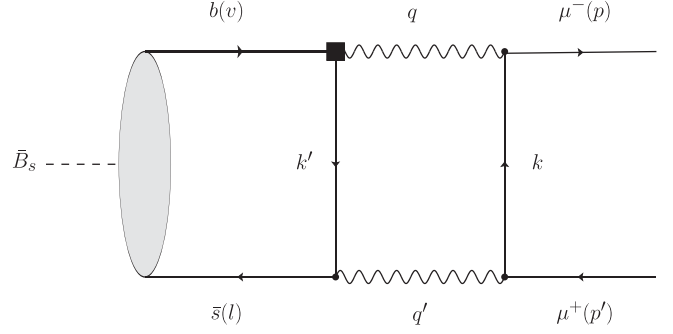

FIG. 1. QED box diagram describing the leading contribution of the operator $\mathcal{O}_7$ (indicated by the black square) to the $\bar{B}_s \rightarrow \mu^+\mu^-$ decay amplitude. The analogous diagram with the role of μ^+ and μ^- interchanged gives the same result and is not shown.

of the time-ordered product of the quark electromagnetic current $j_{\text{em}}^\mu(x) = \sum_q Q_q \bar{q}(x)\gamma^\mu q(x)$ and the effective weak Hamiltonian $\mathcal{H}_{\text{eff}}$, of which we adopt the convention of Ref. [37] and of which the operator

$$\mathcal{O}_7 = \frac{e}{16\pi^2} m_b (\bar{s}_L \sigma^{\mu\nu} b_R) F_{\mu\nu}$$

is our focus in this article. The leading-order contribution of $\mathcal{O}_7$ to the $\bar{B}_s \rightarrow \mu^+\mu^-$ decay amplitude via the nonlocal matrix element (1) is diagrammatically shown in Fig. 1, where an additional virtual photon connects the spectator quark of the $\bar{B}_s$ meson to one of the final-state leptons. The contribution of this diagram (and the corresponding crossed one with the role of the two muons interchanged, which turns out to give the identical contribution) to the $\bar{B}_s \rightarrow \mu^+\mu^-$ decay amplitude was first calculated in Ref. [19] and can be written as

$$i\mathcal{M}(\bar{B}_s \rightarrow \mu^+\mu^-)\Big|_{\mathcal{O}_7}^{\text{LO}} = -\frac{\alpha}{2\pi} Q_\ell^2 Q_s C_7^{\text{eff}} m M f_{B_s}$$
$$\times \mathcal{N}[\bar{u}(p)(1+\gamma_5)v(p')]\mathcal{F}^{\text{LO}}(E, m), \tag{2}$$

with

$$\mathcal{N} = V_{tb}V_{ts}^* \frac{4G_F}{\sqrt{2}} \frac{\alpha}{4\pi} \tag{3}$$

and

$$\mathcal{F}^{\text{LO}}(E, m) = \int_0^\infty \frac{d\omega}{\omega} \phi_+(\omega) \left[\frac{1}{2}\ln^2\frac{m^2}{2E\omega} + \ln\frac{m^2}{2E\omega} + \frac{\pi^2}{3}\right]. \tag{4}$$

Here m denotes the muon mass, $M = m_{B_s} \simeq m_b$ the mass of the $\bar{B}_s$ meson, and $E \simeq M/2$ the muon energy in the

$\bar{B}_s$ meson rest frame. The fermion electric charge fractions are given by $Q_\ell = -1$ and $Q_s = -1/3$.

In Ref. [19] it has been pointed out that the strange-quark propagator in the box diagram leads to a power-enhancement compared to the leading contribution from the local $b \to s\ell^+\ell^-$ operator $\mathcal{O}_{10}$. Furthermore, the propagator depends on the light-cone momentum fraction ω of the initial $\bar{s}$-quark in the $\bar{B}_s$ meson, and consequently the result involves a convolution with the hadronic light-cone distribution amplitude $\phi_+(\omega)$. Most importantly for our work, the form-factor $\mathcal{F}$ turns out to receive a double-logarithmic enhancement which can be traced back to endpoint divergences appearing in the convolution integrals from individual momentum regions, which we discuss in detail in the following.

A. Kinematics

We first fix the notation for the relevant kinematic variables. The momenta of the muons in the final state are used to define two light-cone vectors n^μ and $\bar{n}^\mu$, such that

$$\text{outgoing } \mu^-\colon \; p^\mu = (\bar{n} \cdot p)\frac{n^\mu}{2} + \frac{m^2}{(\bar{n} \cdot p)}\frac{\bar{n}^\mu}{2},$$

$$\text{outgoing } \mu^+\colon \; p'^\mu = (n \cdot p')\frac{\bar{n}^\mu}{2} + \frac{m^2}{(n \cdot p')}\frac{n^\mu}{2}, \quad (5)$$

and the momentum of the incoming $\bar{B}_s$-meson given by

$$Mv^\mu = M\left(\frac{n^\mu}{2} + \frac{\bar{n}^\mu}{2}\right). \quad (6)$$

Here $n^2 = \bar{n}^2 = 0$ and $n \cdot \bar{n} = 2$. The energy E of the muons in the $\bar{B}_s$-meson rest frame is approximately given by the relation $(\bar{n} \cdot p) = (n \cdot p') \simeq 2E = M$. In the diagram

in Fig. 1, the incoming b-quark is described as a static quark in heavy-quark effective theory, characterized by a momentum $p_b^\mu = m_b v^\mu + \Delta^\mu$, with a residual momentum Δ^μ of order Λ_{QCD}. The momentum of the incoming $\bar{s}$-quark is decomposed as

$$\text{incoming } \bar{s}\text{-quark}\colon \; l^\mu = (\bar{n} \cdot l)\frac{n^\mu}{2} + l_\perp^\mu + (n \cdot l)\frac{\bar{n}^\mu}{2}, \quad (7)$$

where here and in the following we neglect the strange-quark mass. It turns out that in the above diagram only the projection $\omega \equiv (\bar{n} \cdot l)$ of the $\bar{s}$-quark in the $\bar{B}_s$-meson enters at leading approximation, which therefore is identified as the argument of the light-cone distribution amplitude in Eq. (4). The ratio of $(\bar{n} \cdot p')$ and $(\bar{n} \cdot l)$ defines the relevant small expansion parameter which we denote as

$$\lambda^2 = \frac{m^2}{2E\omega} \sim \mathcal{O}\left(\frac{\Lambda_{\text{QCD}}}{m_b}\right) \sim \mathcal{O}\left(\frac{m}{m_b}\right), \quad (8)$$

where the muon mass m and the light-cone projection ω of the light spectator-quark momentum are both counted to be of the order of the intrinsic QCD scale Λ_{QCD}, which defines the *soft* scale in the process. The energy of the muons, $E \simeq M/2$, defines the *hard* scale in the process. The product $(2E\omega)$ appears in the denominator of the strange-quark propagator (see below), and thus $\sqrt{2E\omega}$ defines the *hard-collinear* scale in the process.

B. Momentum regions and different choices of analytic regulators

We characterize the external and internal momenta by the scaling of the light-cone projections and the transverse components, using a shorthand notation, e.g.,

$$p^\mu \longleftrightarrow \frac{1}{2E}(\bar{n} \cdot p, p_\perp, n \cdot p) \sim (1, \lambda^2, \lambda^4) \qquad \text{for collinear modes}, \quad (9)$$

$$p'^\mu \longleftrightarrow \frac{1}{2E}(\bar{n} \cdot p', p'_\perp, n \cdot p') \sim (\lambda^4, \lambda^2, 1) \qquad \text{for anticollinear modes}, \quad (10)$$

$$l^\mu \longleftrightarrow \frac{1}{2E}(\bar{n} \cdot l, l_\perp, n \cdot l) \sim (\lambda^2, \lambda^2, \lambda^2) \qquad \text{for soft modes}. \quad (11)$$

The presence of endpoint-divergent integrals requires the introduction of an additional regulator, since dimensional regularization alone is not sufficient. Depending on the additional regulator, one then identifies different sets of relevant momentum regions. In what follows, we compare two different choices for an analytic regulator,

$$\text{option (a)}\colon \; \mathcal{R}_a(k) = \left(\frac{\nu^2}{-(n \cdot k)(\bar{n} \cdot l) + i0}\right)^\delta, \quad (12)$$

$$\text{option (b)}\colon \; \mathcal{R}_b(k) = \left(\frac{\nu^2}{(\bar{n} \cdot k)(n \cdot p') - (n \cdot k)(\bar{n} \cdot l) + i0}\right)^\delta, \quad (13)$$

which are assigned to a muon propagator with momentum k. These regulators are a generalization of the corresponding options discussed—for instance—in Ref. [33] (see also references therein) written in a manifestly boost-invariant form, using the external momenta $(\bar{n} \cdot l)$ and $(n \cdot p')$.

TABLE I. Momentum regions contributing to the box diagram in Fig. 1. Here, $\overline{hc}$, $\bar{c}$, s, and $\overline{sc}$ denote the anti-hard-collinear, anticollinear, soft, and anti-soft-collinear regions, respectively. Notice that the anti-soft-collinear region yields scaleless integrals if the analytic regulator $\mathcal{R}_a$ is used.

Region	Muon	Upper photon	$\bar{s}$-quark	Lower photon	Regulator
$\overline{hc}$	$k \sim (\lambda^2, \lambda, 1)$	$q \sim (1, \lambda, 1)$	$k' \sim (\lambda^2, \lambda, 1)$	$q' \sim (\lambda^2, \lambda, 1)$	$\mathcal{R}_{a,b}$
$\bar{c}$	$k \sim (\lambda^4, \lambda^2, 1)$	$q \sim (1, \lambda^2, 1)$	$k' \sim (\lambda^2, \lambda^2, 1)$	$q' \sim (\lambda^4, \lambda^2, 1)$	$\mathcal{R}_{a,b}$
s	$k \sim (\lambda^2, \lambda^2, \lambda^2)$	$q \sim (1, \lambda^2, \lambda^2)$	$k' \sim (\lambda^2, \lambda^2, 1)$	$q' \sim (\lambda^2, \lambda^2, 1)$	$\mathcal{R}_{a,b}$
$\overline{sc}$	$k \sim (\lambda^3, \lambda^2, \lambda)$	$q \sim (1, \lambda^2, \lambda)$	$k' \sim (\lambda^2, \lambda^2, 1)$	$q' \sim (\lambda^3, \lambda^2, 1)$	$\mathcal{R}_b$

The nonvanishing momentum regions for the box diagram in Fig. 1 are summarized in Table I. Here the momenta of the upper and lower photon lines are given by

$$q^\mu = (p - k)^\mu, \qquad q'^\mu = (p' + k)^\mu, \qquad (14)$$

and the intermediate strange-quark propagator has momentum

$$k'^\mu = (p' + k - l)^\mu. \qquad (15)$$

We observe that in all relevant regions the intermediate strange quark has anti-hard-collinear virtuality, $(k')^2 \sim \lambda^2$, with

$$k' \sim \begin{cases} (\lambda^2, \lambda, 1) & \text{for } k \text{ anti} - \text{hard} - \text{collinear,} \\ (\lambda^2, \lambda^2, 1) & \text{for } k \text{ soft, anticollinear, or anti} - \text{soft} - \text{collinear.} \end{cases}$$

This implies that in all relevant cases, the strange-quark propagator can effectively be replaced by

$$S_F(k') \simeq i \frac{\bar{n}\!\!\!/}{2} \frac{(n \cdot k')}{(n \cdot k')(\bar{n} \cdot k') + (k'_\perp)^2 + i0}$$
$$\simeq i \frac{\bar{n}\!\!\!/}{2} \frac{(2E + n \cdot k)}{(2E + n \cdot k)(\bar{n} \cdot k - \omega) + k_\perp^2 + i0}, \qquad (16)$$

which further simplifies in the individual momentum regions (see below). Here $(n \cdot k') \sim 2E$ is the large component of the anti-hard-collinear momentum, and the propagator only depends on the light-cone projection $\omega = \bar{n} \cdot l$ of the strange-quark momentum in the $\bar{B}_s$ meson.

Inserting this approximation into the box diagram and performing the Lorentz contractions and Dirac projections, and exploiting the equations of motion for the external muon states, we find that the problem reduces to analyzing the scalar integral

$$I(\omega) = \int d(\bar{n} \cdot k) \int d(n \cdot k) \int \widetilde{dk_\perp}$$
$$\cdot \frac{1}{(p - k)^2 + i0} \cdot \frac{1}{(p' + k)^2 + i0}$$
$$\times \frac{(2E + n \cdot k)2E\omega}{(2E + n \cdot k)(\bar{n} \cdot k - \omega) + k_\perp^2 + i0}$$
$$\cdot \frac{2E + n \cdot k}{(n \cdot k)(\bar{n} \cdot k) + k_\perp^2 - m^2 + i0}\Big|_{\text{leading power}}. \qquad (17)$$

The integral measure for the transverse loop momentum reads

$$\widetilde{dk_\perp} = \frac{i\mu^{2\epsilon} e^{\epsilon \gamma_E}}{2\pi^{D/2}} d^{D-2}k_\perp,$$

such that

$$\mathcal{F}^{\text{LO}}(E, m) = \int_0^\infty \frac{d\omega}{\omega} \phi_+(\omega) I(\omega), \qquad (18)$$

where γ_E is the Euler-Mascheroni constant, $D = 4 - 2\epsilon$ denotes the number of space-time dimensions, and μ refers to the $\overline{\text{MS}}$ scale. We now discuss the contributions to the integral $I(\omega)$ from the different momentum regions in turn.

1. The anti-hard-collinear region

The anti-hard-collinear region in the integral (17) is defined by the scaling $k \sim (\lambda^2, \lambda, 1)$, which simplifies the integrand at leading power to

$$I_{\overline{hc}}(\omega) = \int d(\bar{n} \cdot k) \int d(n \cdot k) \int \widetilde{dk_\perp}$$
$$\times \frac{1}{-2E(n \cdot k) + i0} \cdot \frac{1}{(2E + n \cdot k)(\bar{n} \cdot k) + k_\perp^2 + i0}$$
$$\times \frac{(2E + n \cdot k)2E\omega}{(2E + n \cdot k)(\bar{n} \cdot k - \omega) + k_\perp^2 + i0}$$
$$\cdot \frac{2E + n \cdot k}{(n \cdot k)(\bar{n} \cdot k) + k_\perp^2 + i0}. \qquad (19)$$

This integral features an endpoint divergence for $(n \cdot k) \to 0$, which is regularized in $D = 4 - 2\epsilon$ dimensions, such that the analytic regulator can be dropped. Actually, the endpoint divergence arises from the convolution of a hard eikonal propagator (the upper photon) with a remaining jet function consisting of three anti-hard-collinear propagators.

It is convenient to first perform the $(\bar{n} \cdot k)$ integration by residues, and then afterwards the $k_\perp$ integral. This can be written as

$$I_{\overline{hc}}(\omega) = \int_0^1 \frac{du}{u} H_1^{(0)}(u) \bar{J}_1^{(1)}(u; \omega), \qquad (20)$$

where $H_1^{(0)}(u) = 1$ is the leading-order value of the hard matching coefficient for the $b \to s\gamma$ tensor current with an energy transfer $(1 - u)E$, and

$$\bar{J}_1^{(1)}(u; \omega) = -\Gamma(\epsilon) \left(\frac{\mu^2 e^{\gamma_E}}{2E\omega u(1-u)} \right)^\epsilon (1 - u) \qquad (21)$$

is the first nonvanishing term in the jet function associated with the anti-hard-collinear momentum region, with $u \equiv -(n \cdot k)/(n \cdot p')$. Performing the u integral and expanding in ϵ, the result for the anti-hard-collinear region gives

$$I_{\overline{hc}}(\omega) = \frac{1}{\epsilon^2} + \frac{1}{\epsilon} \ln \frac{\mu^2}{2E\omega} + \frac{1}{2} \ln^2 \frac{\mu^2}{2E\omega} - \frac{\pi^2}{12} + \frac{1}{\epsilon} + \ln \frac{\mu^2}{2E\omega} + 2, \qquad (22)$$

which features the standard double logarithms from soft and collinear infrared (IR) divergences, and a single logarithm arising from an endpoint-finite longitudinal integration.

2. The anticollinear region

The anticollinear region in the integral (17) is defined by the scaling $k \sim (\lambda^4, \lambda^2, 1)$, which simplifies the integrand at leading power to

$$I_{\bar{c}}(\omega) = \int d(\bar{n} \cdot k) \int d(n \cdot k) \int \widetilde{dk_\perp} \frac{1}{-2E(n \cdot k) + i0} \cdot \frac{1}{(2E + n \cdot k)(\bar{n} \cdot p' + \bar{n} \cdot k) + k_\perp^2 + i0}$$
$$\times \frac{2E\omega}{-\omega + i0} \cdot \frac{2E + n \cdot k}{(n \cdot k)(\bar{n} \cdot k) + k_\perp^2 - m^2 + i0} \left(\frac{\nu^2}{-\omega(n \cdot k) + i0} \right)^\delta, \qquad (23)$$

with $(\bar{n} \cdot p') = m^2/2E$. This integral now features an endpoint singularity from $(n \cdot k) \to 0$ which is *not* regularized in $D \neq 4$ dimensions due to the nonvanishing mass in the anticollinear muon propagator. In this case the analytic regulator has been kept, and because of the anticollinear scaling of k both variants $\mathcal{R}_a$ and $\mathcal{R}_b$ reduce to the same term as indicated above.

We note that the integral now involves two eikonal propagators. The first one, $(-(\bar{n} \cdot p)(n \cdot k))^{-1}$, reflects the same tree-level hard function from the upper photon propagator as in the anti-hard-collinear region. The second one, $(-\omega)^{-1}$, reflects the tree-level anti-hard-collinear function which decouples from the anticollinear loop integral. Again, we can first perform the $(\bar{n} \cdot k)$ integration by residues, and then the $k_\perp$ integral in $D - 2$ dimensions. The result can be written as

$$I_{\bar{c}}(\omega) = \bar{J}_2^{(0)}(1, \omega) \int_0^1 \frac{du}{u} H_1^{(0)}(u) \bar{C}^{(1)}(u; \omega), \qquad (24)$$

where we have defined the leading-order term in the jet function for the anti-hard-collinear strange-quark propagator with $(\bar{n} \cdot k') = z\omega$,

$$\bar{J}_2^{(0)}(z, \omega) = \frac{1}{z}, \qquad (25)$$

where the overall factor $1/\omega$—that appears in the convolution with the B_s-meson LCDA—has been factored out. The function

$$\bar{C}^{(1)}(u; \omega) = \Gamma(\epsilon) \left(\frac{\mu^2 e^{\gamma_E}}{m^2} \right)^\epsilon \left(\frac{\nu^2}{2E\omega} \right)^\delta (1 - u)^{1-2\epsilon} u^{-\delta} \qquad (26)$$

refers to the leading term of the anticollinear function that describes the recombination process $\mu^+(-k)\gamma(p' + k) \to \mu^+(p')$. Performing the u integration, the final result for the anticollinear region gives

$$I_{\bar{c}}(\omega) = \left(-\frac{1}{\delta} - \ln \frac{\nu^2}{2E\omega} \right) \left(\frac{1}{\epsilon} + \ln \frac{\mu^2}{m^2} \right) + \frac{\pi^2}{3} - \frac{1}{\epsilon} - \ln \frac{\mu^2}{m^2} - 2, \qquad (27)$$

where we first had to expand in δ and subsequently in ϵ. We observe that the anticollinear region depends on the soft momentum ω through the analytic regulator, reflecting the collinear-anomaly phenomenon [38,39].

3. The soft region

The soft region in the integral (17) is defined by the scaling $k \sim (\lambda^2, \lambda^2, \lambda^2)$, which simplifies the integrand at leading power to

$$I_s(\omega) = \int d(\bar{n} \cdot k) \int d(n \cdot k) \int \widetilde{dk_\perp} \cdot \frac{1}{-2E(n \cdot k) + i0}$$
$$\cdot \frac{1}{2E(\bar{n} \cdot k) + i0} \frac{2E\omega}{\bar{n} \cdot k - \omega + i0}$$
$$\cdot \frac{2E}{(n \cdot k)(\bar{n} \cdot k) + k_\perp^2 - m^2 + i0} \mathcal{R}_{a,b}(k), \qquad (28)$$

which is again endpoint divergent and thus requires the additional regulator, as indicated. Let us first consider the analytic regulator for case (b) which, in the soft region, reduces to

$$\mathcal{R}_b(k) \to \left(\frac{\nu^2}{2E(\bar{n} \cdot k) + i0} \right)^\delta,$$

where the $i0$ prescription matches the expression in the respective eikonal photon propagator. In that case, one can first perform the $(n \cdot k)$ integration by residues, and then the $k_\perp$ integral in $D - 2$ dimensions. The soft contribution to the integral then takes the form

$$(b): \quad I_s(\omega) = \Gamma(\epsilon) \left(\frac{\mu^2 e^{\gamma_E}}{m^2} \right)^\epsilon \left(\frac{\nu^2}{2E\omega} \right)^\delta \int\limits_0^\infty dv \frac{(v + i0)^{-1-\delta}}{v - 1 + i0},$$
$$(29)$$

with $v \equiv (\bar{n} \cdot k)/\omega$. The endpoint divergence at $v \to 0$ is regularized by the analytic regulator, while the integral

converges in the ultraviolet (UV), $v \to \infty$. Notice that the integral generates an imaginary part which stems from the situation when the strange-quark propagator goes on shell for $v \to 1$,

$$(b) \quad I_s(\omega) = \left(\frac{1}{\epsilon} + \ln \frac{\mu^2}{m^2} \right) \left(-\frac{1}{\delta} - \ln \frac{\nu^2}{2E\omega} + i\pi \right). \quad (30)$$

On the other hand, taking the analytic regulator for case (a)

$$\mathcal{R}_a(k) \to \left(\frac{\nu^2}{-\omega(n \cdot k) + i0} \right)^\delta,$$

we can first perform the $k_\perp$ integration, to end up with

$$(a) \quad \tilde{I}_s(\omega) = \frac{\Gamma(\epsilon)}{2\pi i} \int \frac{d(n \cdot k)}{-n \cdot k + i0} \int \frac{d(\bar{n} \cdot k)}{\bar{n} \cdot k + i0} \frac{\omega}{\bar{n} \cdot k - \omega + i0}$$
$$\times \left(\frac{\mu^2 e^{\gamma_E}}{-(n \cdot k)(\bar{n} \cdot k) + m^2 - i0} \right)^\epsilon \mathcal{R}_a(k). \quad (31)$$

Now consider the analytic structure in the $(\bar{n} \cdot k)$ plane:
  (i) There are two poles at

$$\mathrm{Re}(\bar{n} \cdot k) = 0, \omega \quad below \text{ the real axis.}$$

  (ii) There is a branch cut from the dimensional regulator,

for $(n \cdot k) > 0$: $m^2/(n \cdot k) \leq \mathrm{Re}(\bar{n} \cdot k)$, $\quad below$ the real axis,

for $(n \cdot k) < 0$: $\mathrm{Re}(\bar{n} \cdot k) \leq m^2/(n \cdot k)$, $\quad above$ the real axis.

For $(n \cdot k) > 0$, the integrand is analytic in the upper half plane, and therefore the integral vanishes. For $(n \cdot k) < 0$, the branch cut from the dimensional regulator is moved to the upper half plane, and by picking up the corresponding discontinuity

$$\mathrm{Disc} \left(\frac{\mu^2}{-(n \cdot k)(\bar{n} \cdot k) + m^2 - i0} \right)^\epsilon = \frac{2\pi i \theta((n \cdot k)(\bar{n} \cdot k) - m^2)}{\Gamma(\epsilon)\Gamma(1 - \epsilon)} \left(\frac{\mu^2}{(n \cdot k)(\bar{n} \cdot k) - m^2} \right)^\epsilon, \qquad (32)$$

we arrive at the representation

$$(a) \quad \tilde{I}_s(\omega) = \frac{1}{\Gamma(1 - \epsilon)} \int\limits_{-\infty}^{0} \frac{d(n \cdot k)}{n \cdot k} \int\limits_{-\infty}^{m^2/n \cdot k} \frac{d(\bar{n} \cdot k)}{\bar{n} \cdot k} \frac{\omega}{\omega - \bar{n} \cdot k} \left(\frac{\mu^2 e^{\gamma_E}}{(n \cdot k)(\bar{n} \cdot k) - m^2} \right)^\epsilon \mathcal{R}_a(k)$$

$$= \frac{1}{\Gamma(1 - \epsilon)} \left(\frac{\mu^2 e^{\gamma_E}}{2E\omega} \right)^\epsilon \left(\frac{\nu^2}{2E\omega} \right)^\delta \int\limits_0^\infty \frac{du}{u} \int\limits_{\lambda^2/u}^\infty \frac{d\rho}{\rho} \frac{1}{1 + \rho} (u\rho - \lambda^2)^{-\epsilon} u^{-\delta}, \qquad (33)$$

where $\rho = -(\bar{n} \cdot k)/\omega$. This can be written as

(a) $\tilde{I}_s(\omega) = H_1^{(0)}(0) \int_0^\infty \frac{du}{u} \int_0^\infty \frac{d\rho}{\rho} S^{(1)}(u, \rho; \omega)$

$$\times \bar{J}_2^{(0)}(1 + \rho, \omega) \tag{34}$$

with the same hard and jet function as already defined above, and a soft function

$$S^{(1)}(u, \rho; \omega) = \theta(u\rho - \lambda^2) \left(\frac{\mu^2 e^{\gamma_E}}{2E\omega} \right)^\epsilon \left(\frac{\nu^2}{2uE\omega} \right)^\delta \frac{(u\rho - \lambda^2)^{-\epsilon}}{\Gamma(1 - \epsilon)}, \tag{35}$$

which stems from the discontinuity of the muon propagator. Performing the longitudinal integrations, we end up with

(a) $\tilde{I}_s(\omega) = \left(\frac{1}{\delta} + \ln \frac{\nu^2}{m^2} \right) \left(\frac{1}{\epsilon} + \ln \frac{\mu^2}{m^2} \right) - \frac{1}{\epsilon^2}$

$$- \frac{1}{\epsilon} \ln \frac{\mu^2}{m^2} - \frac{1}{2} \ln^2 \frac{\mu^2}{m^2} + \frac{\pi^2}{12}. \tag{36}$$

In that case, the full integral is already reproduced by the sum of the anti-hard-collinear, the anticollinear, and the soft region,

(a) $I(\omega) = I_{\overline{hc}}(\omega) + I_{\bar{c}}(\omega) + \tilde{I}_s(\omega)$

$$= \frac{1}{2} \ln^2 \frac{m^2}{2E\omega} + \ln \frac{m^2}{2E\omega} + \frac{\pi^2}{3}. \tag{37}$$

Notice that the single logarithm in this expression stems from the cancellation of single powers of $1/\epsilon$ in the $\overline{hc}$ and $\bar{c}$ region.

4. Anti-soft-collinear region

For the regulator $\mathcal{R}_b$, we also have to take into account an anti-soft-collinear region, where $k^\mu \sim (\lambda^3, \lambda^2, \lambda)$. In this region the integral (17) at leading power reduces to

$$I_{\overline{sc}}(\omega) = \int d(\bar{n} \cdot k) \int d(n \cdot k) \int \widetilde{dk_\perp} \cdot \frac{1}{-2En \cdot k + i0}$$

$$\cdot \frac{1}{2E\bar{n} \cdot k + i0} \frac{4E^2\omega}{-2E\omega + i0}$$

$$\cdot \frac{2E}{(n \cdot k)(\bar{n} \cdot k) + k_\perp^2 - m^2 + i0} \mathcal{R}_b(k). \tag{38}$$

In that case, it is again convenient to first perform the $k_\perp$ integration, which yields

(b) $I_{\overline{sc}}(\omega) = \frac{\Gamma(\epsilon)}{2\pi i} \int \frac{d(n \cdot k)}{n \cdot k - i0} \int \frac{d(\bar{n} \cdot k)}{\bar{n} \cdot k + i0}$

$$\times \left(\frac{\mu^2 e^{\gamma_E}}{-(n \cdot k)(\bar{n} \cdot k) + m^2 - i0} \right)^\epsilon$$

$$\times \left(\frac{\nu^2}{2E(\bar{n} \cdot k) - \omega(n \cdot k) + i0} \right)^\delta. \tag{39}$$

We now consider the analytic structure of the integrand in the complex $(n \cdot k)$ plane.

(i)   There is always a pole at

$$\text{Re}(n \cdot k) = 0, \quad above \text{ the real axis.}$$

(ii)   There is a branch cut from the dimensional regulator,

for $(\bar{n} \cdot k) > 0$: $m^2/(\bar{n} \cdot k) \leq \text{Re}(n \cdot k)$,   *below* the real axis,

for $(\bar{n} \cdot k) < 0$: $\text{Re}(n \cdot k) \leq m^2/(\bar{n} \cdot k)$,   *above* the real axis.

(iii)   There is a branch cut from the rapidity regulator,

$$(n \cdot p')(\bar{n} \cdot k)/\omega \leq \text{Re}(n \cdot k), \quad above \text{ the real axis.}$$

For $(\bar{n} \cdot k) < 0$, the integrand is analytic in the lower half plane, and therefore the integral vanishes. For $(\bar{n} \cdot k) > 0$, the branch cut from the dimensional regulator is moved to the lower half plane, and by picking up the corresponding discontinuity (32), we obtain

(b) $I_{\overline{sc}}(\omega) = \frac{1}{\Gamma(1 - \epsilon)} \int_0^\infty \frac{d(n \cdot k)}{n \cdot k} \int_0^\infty \frac{d(\bar{n} \cdot k)}{\bar{n} \cdot k}$

$$\times \theta((n \cdot k)(\bar{n} \cdot k) - m^2) \tag{40}$$

$$\times \left(\frac{\mu^2 e^{\gamma_E}}{(n \cdot k)(\bar{n} \cdot k) - m^2} \right)^\epsilon \left(\frac{\nu^2}{2E(\bar{n} \cdot k) - \omega(n \cdot k) + i0} \right)^\delta$$

$$= \left(\frac{\mu^2 e^{\gamma_E}}{2E\omega} \right)^\epsilon \left(\frac{\nu^2}{2E\omega} \right)^\delta \int_0^\infty \frac{du'}{u'} \int_0^\infty \frac{dv}{v} \theta(u'v - \lambda^2) \frac{(u'v - \lambda^2)^{-\epsilon}}{\Gamma(1 - \epsilon)}$$

$$\times (v - u' + i0)^{-\delta}, \tag{41}$$

where $u' = -u = (n \cdot k)/2E$ and $v = (\bar{n} \cdot k)/\omega$ as before. This integral can most easily be solved by decomposing it into two terms, one with $v > u'$ and one with $v < u'$. Both integrals are identical, except for an additional phase factor $e^{-i\pi\delta}$ that arises in the second case and effectively amounts to replacing $1/\delta \rightarrow 1/\delta - i\pi$ after expanding in δ. It is also instructive to consider the variable transform $x = v - u'$ and $y = u'v$. Here, the integral over x produces a UV pole

that is regularized by δ, while y produces a UV pole that is regularized by ϵ. The net result is

$$(b) \quad I_{\overline{sc}}(\omega) = \tilde{I}_s(\omega) - I_s(\omega)$$

$$= -\frac{1}{\epsilon^2} - \frac{1}{\epsilon}\ln\frac{\mu^2}{m^2} - \frac{1}{2}\ln^2\frac{\mu^2}{m^2} + \left(\frac{1}{\epsilon} + \ln\frac{\mu^2}{m^2}\right)$$

$$\times \left(\frac{2}{\delta} - i\pi + \ln\frac{\nu^2}{2E\omega} + \ln\frac{\nu^2}{m^2}\right) + \frac{\pi^2}{12}. \quad (42)$$

With this we obtain an alternative decomposition of the form-factor integral

$$(b) \quad I(\omega) = I_{\overline{hc}}(\omega) + I_{\bar{c}}(\omega) + I_s(\omega) + I_{\overline{sc}}(\omega). \quad (43)$$

Notice that the (divergent) imaginary part $i\pi(\frac{1}{\epsilon} + \ln\frac{\mu^2}{m^2})$ cancels between the soft and anti-soft-collinear region. Furthermore, in the $\overline{sc}$ region, the reference scale for the analytic regulator is set by the geometric mean of the anti-hard-collinear scale $\sqrt{2E\omega}$ and the soft scale m.

C. Anti-soft-collinear region with cutoff

The double-logarithmic term in $I(\omega)$ can also be obtained in an alternative manner by considering the IR contribution to the anti-soft-collinear region only (see also the analogous discussion in Refs. [33] or [36] and references therein), where the dimensionless integration variables u, v are cut off from above at their natural value 1,

$$I(\omega)\Big|_{\text{double-log}} = I_{\overline{sc}}\Big|_{\text{cut}} = \int_0^1 \frac{du}{u} \int_0^1 \frac{dv}{v} \theta(uv - \lambda^2)$$

$$= \frac{1}{2}\theta(1 - \lambda^2)\ln^2\lambda^2. \quad (44)$$

Notice that we have kept a theta-function $\theta(1 - \lambda^2)$ here, because $\lambda^2 = \frac{m^2}{2E\omega}$ depends on the integration variable ω, such that *formally* we can have $\lambda^2 > 1$ for $\omega < m^2/2E$. However, in the end, the hadronic parameters in the B_s-meson LCDA respect the power-counting $\omega \sim \Lambda_{\text{QCD}}$, such that we can expand, $\theta(1 - \lambda^2) = 1 + \mathcal{O}(m/E)$. The double-logarithmic term in the form factor for the $\mathcal{O}_7$ contribution can thus be written as

$$\mathcal{F}^{\text{LO}}(E, m)\Big|_{\text{double-log}} = \int \frac{d\omega}{\omega}\varphi_+(\omega) \int_0^1 \frac{du}{u}$$

$$\times \int_0^1 \frac{dv}{v}\theta(2E\omega uv - m^2). \quad (45)$$

For the following discussion it is useful to rewrite the integral over the light-quark momentum ω in the so-called dual space introduced in Ref. [40]:

$$\phi_+(\omega) = \int \frac{d\omega'}{\omega'}\sqrt{\frac{\omega}{\omega'}}J_1\left(2\sqrt{\frac{\omega}{\omega'}}\right)\rho_+(\omega'), \quad (46)$$

with the Bessel function of the first kind J_1. Since the second logarithmic moments of $\phi_+(\omega)$ and $\rho_+(\omega')$ coincide [40], we can as well write the double-logarithmic contribution to the form factor as

$$\mathcal{F}^{\text{LO}}(E, m)\Big|_{\text{double-log}} = \frac{1}{2}\int \frac{d\omega'}{\omega'}\rho_+(\omega')\ln^2\frac{m^2 e^{2\gamma_E}}{2E\omega'}. \quad (47)$$

D. Construction of the factorization theorem

The analysis of the box diagram above determines the form of a bare factorization theorem that takes into account additional QCD corrections from different momentum regions, depending on the regulator being used. For concreteness, we stick to the analytic regulator $\mathcal{R}_a(k)$, such that the anti-soft-collinear region does not appear in the bare factorization theorem. The form factor for the $\mathcal{O}_7$ contribution then decomposes into three additive terms,

$$\mathcal{F}(E, m) = \int_0^\infty \frac{d\omega}{\omega}\phi_+(\omega)\Bigg\{\int_0^1 \frac{du}{u}H_1(u)\bar{J}_1(u; \omega)$$

$$+ \bar{J}_2(1, \omega)\int_0^1 \frac{du}{u}H_1(u)\bar{C}(u; \omega) + H_1(0)$$

$$\times \int_0^\infty \frac{du}{u}\int_0^\infty \frac{d\rho}{\rho}S(u, \rho; \omega)\bar{J}_2(1 + \rho, \omega)\Bigg\}_{\text{bare}}$$

$$(48)$$

where each individual term contains an endpoint-divergent convolution integral that is regularized for finite ϵ and δ. Here

$$H_1(u) = H_1^{(0)}(u) + \mathcal{O}(\alpha_s), \quad (49)$$

$$\bar{J}_1(u; \omega) = \bar{J}_1^{(1)}(u; \omega) + \mathcal{O}(\alpha_s), \quad (50)$$

$$\bar{J}_2(z) = \bar{J}_2^{(0)}(z) + \mathcal{O}(\alpha_s), \quad (51)$$

with $H_1^{(0)}(u) = 1$, and $\bar{J}_1^{(1)}(u; \omega)$, $\bar{J}_2^{(0)}(z)$ given in Eqs. (21) and (25). Notice that in the bare factorization theorem (48) we have not taken into account additional QED corrections to the $\gamma^*\gamma^* \to \mu^+\mu^-$ subprocess, i.e. the collinear and soft functions related to the muon,

$$\bar{C}(u; \omega) = \bar{C}^{(1)}(u; \omega) + \mathcal{O}(\alpha), \quad (52)$$

$$S(u, \rho; \omega) = S^{(1)}(u, \rho; \omega) + \mathcal{O}(\alpha) \quad (53)$$

are set to their leading-order expressions given in Eqs. (26) and (35).

In order to get rid of the analytic regulator in the bare factorization theorem, we have to exploit the

refactorization condition [28,36,40] for the anticollinear function. Following the notation of [36], we define

$$[[\bar{C}(u;\omega)]] \equiv \bar{C}(u;\omega)|_{u\to 0} = \int_0^\infty \frac{d\rho}{\rho} S(u,\rho;\omega) + \mathcal{O}(\alpha) \quad (54)$$

which in our case provides a trivial identity between the QED fixed-order expressions in (26) and (35). In addition,

we use that in case of analytic regulators the scaleless double integral

$$\int_0^\infty \frac{du}{u} \int_0^\infty \frac{d\rho}{\rho} S(u,\rho;\omega) = 0, \quad (55)$$

vanishes. As described in detail in the Appendix, the factorization can then be rearranged as follows:

$$\mathcal{F}(E,m) = \int_0^\infty \frac{d\omega}{\omega} \phi_+(\omega) \Bigg\{ \int_0^\infty \frac{du}{u} \Bigg[H_1(u) \bar{J}_1(u;\omega) \theta(1-u) - H_1(0) \bar{J}_2(1,\omega) \theta(u-1) \int_1^\infty \frac{d\rho}{\rho} S(u\rho;\omega) \Bigg]_{\lambda^2 \to 0}$$

$$+ \bar{J}_2(1,\omega) \int_0^1 \frac{du}{u} [H_1(u)\bar{C}(u) - H_1(0)[[\bar{C}(u)]]] + H_1(0) \int_0^\infty \frac{du}{u} \int_0^\infty \frac{d\rho}{\rho} [\bar{J}_2(1+\rho,\omega) - \theta(1-\rho)$$

$$\times \bar{J}_2(1,\omega)] S(u\rho;\omega) + \bar{J}_2(1,\omega) H_1(0) \int_0^1 \frac{du}{u} \int_0^1 \frac{d\rho}{\rho} S(u\rho;\omega)|_{\lambda^2 \to 0} \Bigg\}, \quad (56)$$

where now the limit $\delta \to 0$ can be performed *before* the integrations, and therefore the anticollinear function does not depend on ω anymore, and the soft function only depends on the product $u\rho$ (and, via the dimensional regulator, on ω). Comparison with the bare factorization theorem shows that now all endpoint divergences are subtracted from the anti-hard-collinear, anticollinear, and soft momentum regions. The endpoint logarithms are fully contained in the fourth term which coincides with the expression obtained from the anti-soft-collinear region with explicit momentum cutoffs, see Eq. (44) above. Notice that the emerging cutoffs in the first and fourth terms of the r.h.s. of Eq. (56) lead to additional power corrections in λ^2 which should be dropped, as indicated by the limit $\lambda^2 \to 0$. The factorization theorem in Eq. (56) represents one of the main results of our paper. The various functions appearing in Eq. (56) can now be associated with effective operators in soft-collinear effective theory (SCET) which can be renormalized in a standard manner *before* the convolution integrals are performed. However, a detailed proof of the factorization theorem along these lines is beyond the scope of this work. We should also stress that despite the fact that the structure of our factorization theorem allows us to systematically include QCD corrections, it does not capture the effect of additional QED corrections. In particular, the latter would also modify the refactorization condition (54), and the QED corrections to the B_s-meson LCDA have to be taken into account as well [24].

III. LEADING-LOGARITHMIC QCD CORRECTIONS

In the previous section we have identified the relevant momentum configuration for the virtual muon in the QED box diagram that is responsible for the double-logarithmic enhancement. On top of these endpoint logarithms, we can now include the leading-logarithmic QCD corrections to

the $\bar{B}_s \to \gamma^*\gamma^*$ subprocess within the very same momentum configuration. A similar line of reasoning can be found, for instance, in Ref. [41] for bottom-induced $h \to \gamma\gamma$ decays. Here the LO triangle diagram also contains a double-logarithmic enhancement from the endpoint configuration of the bottom-quark propagator between the two external photons. In that case, the leading double-logarithmic corrections can be included by dressing the off-shell $h \to b^*\bar{b}^*$ vertex with a standard QCD Sudakov form factor. Notice that the systematic resummation of large logarithms $\ln m_b/m_h$ for this process on the basis of RG equations in SCET has been developed only recently in Refs. [30,31].

At one-loop accuracy the RG evolution is multiplicative in dual space, and—restricting ourselves to the anti-soft-collinear region which generates the leading double-logarithmic term in Eq. (47)—we can include the leading logarithmic radiative QCD corrections from hard, anti-hard-collinear, and soft QCD effects simply via the factorization formula

$$\mathcal{F}(E,m)\Big|_{\mathrm{LL}} = \frac{1}{2} H_1(0;\mu) \int \frac{d\omega'}{\omega'} \rho_+(\omega';\mu) \ln^2 \frac{m^2 e^{2\gamma_E}}{2E\omega'}$$

$$\times \bar{\mathcal{J}}_2(1,\omega';\mu), \quad (57)$$

where $H_1(0,\mu)$ includes the leading-logarithmic (LL) running of the hard matching coefficient for the $b \to s\gamma^*$ vertex, and $\bar{\mathcal{J}}_2(1,\omega',\mu)$ the corresponding expression for the anti-hard-collinear jet function in dual space. The dual LCDA $\rho_+(\omega',\mu)$ includes the scale dependence from soft QCD modes. This is illustrated in Fig. 2. The μ dependence between the individual terms in Eq. (57) has to drop out. We now discuss the individual terms in turn.
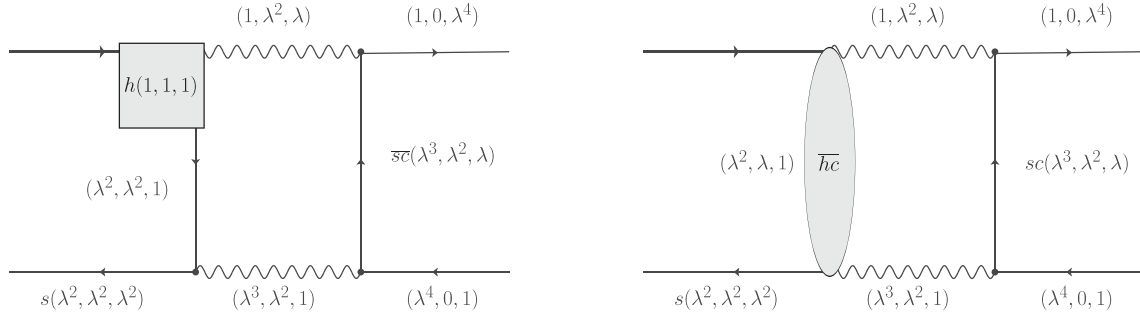
FIG. 2. Illustration of short-distance QCD corrections to the anti-soft-collinear region. Left: hard correction to $b \to s\gamma^*$ vertex. Right: anti-hard-collinear corrections to spectator scattering.

A. Hard QCD corrections at the $b \to s\gamma^*$ vertex

The hard corrections to the Wilson coefficients of heavy-to-light currents have been calculated in the framework of SCET, see for instance Ref. [42]. In the double-logarithmic approximation, we would only have to take into account the leading universal term in the corresponding solution to the RG equation,

$$
\begin{aligned}
H_1(0;\mu) &= e^{V(\mu,\mu_h)} \left(\frac{\mu_h}{2E}\right)^{-g(\mu,\mu_h)} H_1(0;\mu_h) \\
&\simeq \exp\left[-\frac{4\pi C_F}{b_0^2 \alpha_s(\mu_h)}\left(\frac{1}{z_h} - 1 + \ln z_h\right)\right. \\
&\quad \left. + \frac{2C_F}{b_0}\ln\frac{\mu_h}{2E}\ln z_h\right] H_1(0;\mu_h),
\end{aligned}
\tag{58}
$$

with $C_F = 4/3$,

$$
z_h = z(\mu,\mu_h) = \frac{\alpha_s(\mu)}{\alpha_s(\mu_h)} \simeq \frac{2\pi}{2\pi + b_0\alpha_s(\mu_h)\ln\frac{\mu}{\mu_h}}
\tag{59}
$$

and $b_0 = 11 - 2n_f/3$ being the leading coefficient in the QCD beta function. The above formula resums all terms of order $\alpha_s^n \ln^{2n}\frac{\mu}{\mu_h}$. The matching scale μ_h should be identified with twice the energy of the virtual photon, which in the anti-soft-collinear region equals the muon energy:

$$
\mu_h = (\bar{n} \cdot p) \simeq 2E
$$

such that $H_1(0;\mu_h) = 1 + \mathcal{O}(\alpha_s)$ without logarithmically enhanced terms, and

$$
H_1(0;\mu) = e^{V(\mu,2E)} H_1(0;\mu_h = 2E).
$$

B. Soft corrections to the B-meson LCDA

The B-meson LCDA in dual space renormalizes multiplicatively at one-loop accuracy [40],

$$
\rho_+(\omega',\mu) = e^{V(\mu,\mu_0)} \left(\frac{\mu_0 e^{2\gamma_E}}{\omega'}\right)^{-g(\mu,\mu_0)} \rho_+(\omega',\mu_0),
\tag{60}
$$

where $V(\mu,\mu_0)$ is defined analogously as before, with $\mu_h \to \mu_0$, and

$$
g(\mu,\mu_0) \simeq -\frac{2C_F}{b_0}\ln z_s
\tag{61}
$$

to leading-logarithmic accuracy, with

$$
z_s = z(\mu,\mu_0) = \frac{\alpha_s(\mu)}{\alpha_s(\mu_0)}.
\tag{62}
$$

The scale μ_0 refers to a soft reference scale where a model/parametrization of the LCDA is defined. Throughout this article, we set $\mu_0 = 1$ GeV.

C. Hard-collinear corrections to the strange-quark jet function

Following the discussion around (2.33) in Ref. [40], the leading logarithmic corrections to the jet function describing the corrections to the strange-quark exchange in the anti-hard-collinear scattering process in dual space is again described by a multiplicative renormalization factor,

$$
\bar{\mathcal{J}}_2(1,\omega';\mu) = e^{-2V(\mu,\mu_{hc})} \left(\frac{\mu_{hc}^2 e^{2\gamma_E}}{2E\omega'}\right)^{g(\mu,\mu_{hc})} \bar{\mathcal{J}}_2(1,\omega';\mu_{hc}),
\tag{63}
$$

with the same RG functions V and g as above.

D. Net result for RG-improved endpoint contribution

Combining all RG factors, the dependence on the factorization scale μ drops out in the product

$$e^{V(\mu,2E)}\mathcal{J}(2E\omega',\mu)e^{V(\mu,\mu_0)}\left(\frac{\hat{\mu}_0}{\omega'}\right)^{-g(\mu,\mu_0)}$$

$$= e^{V(\mu_{hc},\mu_h)}e^{V(\mu_{hc},\mu_0)}\left(\frac{\hat{\mu}_0}{\omega'}\right)^{-g(\mu_{hc},\mu_0)},$$

as required [43]. Here we abbreviate $\hat{\mu}_0 = \mu_0 e^{2\gamma_E}$, and identify $\mu_h = 2E$, as well as $\bar{\mathcal{J}}_2(1,\omega';\mu_{hc}) \simeq 1$. Inserting the net leading-logarithmic RG factor into the form factor for the $\mathcal{O}_7$ contribution, we end up with

$$\mathcal{F}(E,m)\Big|_{\mathrm{LL}} = \frac{1}{2}e^{V(\mu_{hc},\mu_h)}e^{V(\mu_{hc},\mu_0)}\int\frac{d\omega'}{\omega'}\ln^2\frac{m^2}{2E\hat{\omega}'}$$
$$\times\left(\frac{\hat{\mu}_0}{\omega'}\right)^{-g(\mu_{hc},\mu_0)}\rho_+(\omega',\mu_0), \qquad (64)$$

with $\hat{\omega}' = \omega' e^{-2\gamma_E}$. If we define the generating function for logarithmic moments of $\rho_+(\omega',\mu_0)$ as [40]

$$F_{[\rho_+]}(t;\mu_0,\mu_m) = \int_0^\infty\frac{d\omega'}{\omega'}\left(\frac{\hat{\mu}_m}{\omega'}\right)^{-t}\rho_+(\omega',\mu_0), \qquad (65)$$

this can also be written as $(\hat{\mu}_m = \mu_m e^{2\gamma_E})$

$$\mathcal{F}(E,m)\Big|_{\mathrm{LL}} = \frac{1}{2}e^{V(\mu_{hc},\mu_h)}e^{V(\mu_{hc},\mu_0)}\left(\frac{2E\mu_0}{m^2}\right)^{-g(\mu_{hc},\mu_0)}\frac{d^2}{dt^2}$$
$$\times F_{[\rho_+]}\left(t + g(\mu_{hc},\mu_0);\mu_0,\frac{m^2}{2E}\right)\Big|_{t=0}. \qquad (66)$$

The compact formulas for the form factor contain the leading double-logarithmic enhancement from the endpoint configuration of the muon propagator, supplemented by the leading-logarithmic QCD corrections in RG-improved perturbation theory. As such they still depend on the shape of the B_s-meson LCDA or its generating function for

logarithmic moments. Thus, for numerical studies one has to consider models or generic parametrizations for $\rho_+(\omega')$ or $F_{[\rho_+]}(t)$ at the soft reference scale μ_0 which is the subject of the next subsection.

E. Explicit parametrization of the B_s-meson LCDA and numerical estimates

With the compact expression for the form factor at hand, we can use an explicit but general parametrization of the LCDA as suggested in Ref. [44]:

$$\rho_+(\omega',\mu_0) = \frac{e^{-\omega_0/\omega'}}{\omega'}\sum_{k=0}^K\frac{(-1)^k a_k(\mu_0)}{1+k}L_k^{(1)}(2\omega_0/\omega'), \quad (67)$$

where $L_k^{(1)}$ are associated Laguerre polynomials. The logarithmic moments of $\rho_+(\omega')$ for this parametrization can be obtained as derivatives of the generating function:

$$F_{[\rho_+]}(t;\mu_0,\mu_m) = \frac{\Gamma(1-t)}{\omega_0}\left(\frac{\hat{\mu}_m}{\omega_0}\right)^{-t}$$
$$\times\sum_{k=0}^K a_k(\mu_0)\,_2F_1(-k,1+t;2;2), \quad (68)$$

where the hypergeometric functions with a negative integer $-k$ as their first argument are polynomials of order k,

$$\,_2F_1(0,1+t;2;2) = 1,$$
$$\,_2F_1(-1,1+t;2;2) = -t,$$
$$\,_2F_1(-2,1+t;2;2) = \frac{1}{3}(1+2t^2)\quad\text{etc.} \qquad (69)$$

Truncating the parametrization for $\rho_+(\omega',\mu_0)$ at $K = 2$, we obtain

$$\mathcal{F}(E,m)\Big|_{\mathrm{LL}} \simeq \frac{\Gamma(1-g)}{2\omega_0}e^{V(\mu_{hc},\mu_h)+V(\mu_{hc},\mu_0)}\left(\frac{\hat{\mu}_0}{\omega_0}\right)^{-g}\left\{\left(a_0 - ga_1 + \frac{1+2g^2}{3}a_2\right)[(\ln\hat{\lambda}_0^2 + \psi(1-g))^2 + \psi'(1-g)]\right.$$
$$\left. + \left(2a_1 - \frac{8}{3}ga_2\right)(\ln\hat{\lambda}_0^2 + \psi(1-g)) + \frac{4a_2}{3}\right\}$$
$$\equiv \sum_{k=0}^2 a_k f_k(\omega_0), \qquad (70)$$

where ψ is the digamma function, $a_k = a_k(\mu_0)$, $g = g(\mu_{hc},\mu_0)$, and we defined the abbreviation

$$\hat{\lambda}_0^2 \equiv \frac{m^2 e^{2\gamma_E}}{2E\omega_0}.$$

To illustrate the numerical effect of the RG improvement, we consider $\mu_0 = 1$ GeV, $\mu_h = 5.3$ GeV,

$\mu_{hc} = \sqrt{\mu_h\mu_0} \simeq 2.3$ GeV, with the following values of the strong coupling at the individual scales:

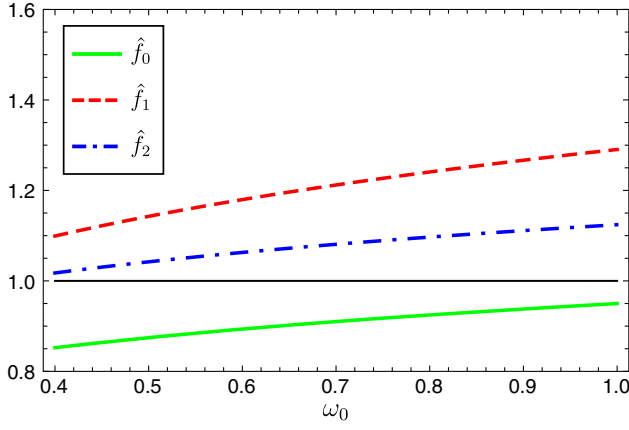$$\alpha_s(\mu_0) = 0.49, \qquad \alpha_s(\mu_h) \simeq 0.21,$$

leading to

FIG. 3. For illustration of the RG effect, we plot the prefactors in front of the expansion coefficients a_k defined in Eq. (70) as a function of the auxiliary scale ω_0 and normalized to the case $g = V = 0$, which we call $\hat{f}_k(\omega_0) \equiv \frac{f_k(\omega_0)}{f_k(\omega_0)|_{g=V=0}}$, for $k = 0, 1, 2$.

$$z(\mu_{hc}, \mu_h) = 1.30, \qquad z(\mu_{hc}, \mu_0) = 0.65,$$

for $n_f = 4$, which yields

$$g \simeq 0.138 \quad \text{and} \quad V(\mu_{hc}, \mu_h) \simeq -0.037,$$
$$V(\mu_{hc}, \mu_0) \simeq -0.053.$$

for the relevant RG functions. From Fig. 3 we see that the RG effect can be as large as $(-15, +30, +10)\%$ for the contributions of the coefficients $a_{0,1,2}$, respectively, depending on the value of the auxiliary scale ω_0 in the parametrization of the B_s-meson LCDA. Notice that the ω_0 dependence of the RG effect is dominated by the factor $(\hat{\mu}_0/\omega_0)^{-g}$ in Eq. (70).

The leading-logarithmic QCD corrections to the $\mathcal{O}_7$ contribution have also been outlined in Ref. [20] where the additional approximation

$$e^{V(\mu_{hc}, \mu_0)} \int \frac{d\omega'}{\omega'} \ln^2 \frac{m^2}{2E\hat{\omega}'} \left(\frac{\hat{\mu}_0}{\omega'}\right)^{-g} \rho_+(\omega', \mu_0)$$

$$\to \frac{e^{V(\mu_{hc}, \mu_0)} \int \frac{d\omega'}{\omega'} \left(\frac{\hat{\mu}_0}{\omega'}\right)^{-g} \rho_+(\omega', \mu_0)}{\int \frac{d\omega'}{\omega'} \rho_+(\omega', \mu_0)}$$

$$\cdot \left[\int \frac{d\omega'}{\omega'} \ln^2 \frac{m^2}{2E\hat{\omega}'} \rho_+(\omega', \mu_0)\right]$$

$$= \frac{\lambda_{B_s}(\mu_0)}{\lambda_{B_s}(\mu_{hc})} \int \frac{d\omega'}{\omega'} \ln^2 \frac{m^2}{2E\hat{\omega}'} \rho_+(\omega', \mu_0) \qquad (71)$$

has been used, which is formally valid since

$$\ln^2 \frac{m^2}{2E\hat{\omega}'} = \ln^2 \frac{m^2}{2E\hat{\omega}_0} + \text{subleading logs},$$

as long as $\omega_0 \sim \Lambda_{\rm QCD}$. For the numerical estimate of the scale dependence of the first inverse moment $\lambda_{B_s}^{-1}$ of the B_s-meson LCDA, the authors of Ref. [20] employed the simple exponential model that corresponds to taking $a_0 = 1$ and $a_{k>0} = 0$ in the generic parametrization (67). Adopting these additional simplifications and using otherwise the same numerical input as quoted above, we find about (-15%) to (-30%) reduction—depending on the value of ω_0—from the leading-logarithmic QCD corrections to the form factor $\mathcal{F}$. Up to numerical differences related to the treatment of α_s and the implementation of the RG evolution of $\lambda_{B_s}(\mu)$ [45], this is in line with the numerical estimate in Ref. [20]. We also observe that without the approximation (71) the RG effect on the a_0 contribution captured by the function $\hat{f}_0$, as illustrated by the green solid line in Fig. 3, is slightly reduced.

IV. SUMMARY

We have studied the factorization of QCD effects for the contribution of the electromagnetic dipole operator $\mathcal{O}_7$ to the $\bar{B}_s \to \mu^+\mu^-$ decay amplitude. This arises from the nonlocal hadronic matrix element in Eq. (1). To this end, we have first performed a careful reanalysis of the leading QED box diagram using the method of momentum regions with two different options for an analytic regulator that has to be introduced to handle the otherwise divergent convolution integrals. In particular, we identified the relevant momentum region that is responsible for the double-logarithmic enhancement in the small ratio of soft and hard scales in the process. Considering the bare QCD factorization theorem that captures the different momentum regions for a given regulator, we performed the necessary subtractions to render all convolution integrals finite, such that the integrands can be renormalized in the standard manner. The so-obtained factorization theorem allows one to include radiative QCD corrections in renormalization-group improved perturbation theory. Focusing on the kinematic configuration that is responsible for the double-logarithmic enhancement, we included the leading-logarithmic QCD corrections in a straightforward manner by taking into account the RG evolution for the hard, soft, and jet function describing the relevant decay of the $\bar{B}_s$-meson to two (virtual) photons in QCD factorization. The leading-logarithmic RG factor takes a particularly simple form in the so-called dual space for the light-cone distribution amplitude of the $\bar{B}_s$-meson. We find a compact analytic expression on the basis of a systematic parametrization of the B_s-meson's two-particle LCDA. Numerically, the effect of the leading-logarithmic QCD corrections turns out to be up to 30% relative to the $\mathcal{O}_7$ contribution at fixed-order $\mathcal{O}(\alpha_s^0)$, in qualitative agreement with an earlier estimate in Ref. [20]. We remind the reader that the net contribution of $\mathcal{O}_7$ to the total $\bar{B}_s \to \mu^+\mu^-$ rate is, however, small. From the theoretical point of view it

would be interesting to confirm our findings by an explicit two-loop calculation including all combinations of momentum regions, which we leave for future investigation.

APPENDIX: DETAILED DERIVATION OF THE FACTORIZATION THEOREM

In this appendix we give a detailed derivation of the factorization theorem Eq. (56), by specifying the necessary subtractions that make every single convolution integral finite. The starting point is the bare factorization theorem for the analytic regulator $\mathcal{R}_a(k)$ in Eq. (48),

$$
\mathcal{F}(E, m) = \int_0^\infty \frac{d\omega}{\omega} \phi_+(\omega) \left\{ \int_0^1 \frac{du}{u} H_1(u) \bar{J}_1(u; \omega) \right.
$$
$$
+ \bar{J}_2(1, \omega) \int_0^1 \frac{du}{u} H_1(u) \bar{C}(u; \omega) + H_1(0)
$$
$$
\left. \times \int_0^\infty \frac{du}{u} \int_0^\infty \frac{d\rho}{\rho} S(u, \rho; \omega) \bar{J}_2(1 + \rho, \omega) \right\}_{\text{bare}}.
$$

The procedure to perform the subtractions of endpoint divergences in the convolution integrals follows closely the analysis in Ref. [36]. However, in our case the situation is somewhat simpler, because some of the functions are only needed at leading order, as long as QED corrections of order $\mathcal{O}(\alpha)$ are ignored.

By means of the refactorization condition (54) we can rearrange the divergent convolution integral in the second line of the factorization theorem as follows:

$$
\bar{J}_2(1, \omega) \int_0^1 \frac{du}{u} H_1(u) \bar{C}(u; \omega)
$$
$$
= \bar{J}_2(1, \omega) H_1(0) \int_0^1 \frac{du}{u} \int_0^\infty \frac{d\rho}{\rho} S(u, \rho; \omega)
$$
$$
+ \bar{J}_2(1, \omega) \int_0^1 \frac{du}{u} [H_1(u) \bar{C}(u; \omega) - H_1(0)[[C(u; \omega)]]]
$$

$$(A1)$$

where the integral in the last line does not contain an endpoint divergence anymore. Similarly, in the last

term of the bare factorization, we first decompose the ρ integral as [47]

$$
H_1(0) \int_0^\infty \frac{du}{u} \int_0^\infty \frac{d\rho}{\rho} \bar{J}_2(1 + \rho, \omega) S(u, \rho; \omega)
$$
$$
= H_1(0) \int_0^\infty \frac{du}{u} \int_0^1 \frac{d\rho}{\rho} \bar{J}_2(1 + \rho, \omega) S(u, \rho; \omega)
$$
$$
+ H_1(0) \int_0^\infty \frac{du}{u} \int_1^\infty \frac{d\rho}{\rho} \bar{J}_2(1 + \rho, \omega) S(u, \rho; \omega), \quad (A2)
$$

where the first term on the right-hand side contains the $1/\delta$ divergence, while the second term is finite in the limit $\delta \to 0$. The former can be further decomposed

$$
H_1(0) \int_0^\infty \frac{du}{u} \int_0^1 \frac{d\rho}{\rho} \bar{J}_2(1 + \rho, \omega) S(u, \rho; \omega)
$$
$$
= H_1(0) \int_0^\infty \frac{du}{u} \int_0^1 \frac{d\rho}{\rho} (\bar{J}_2(1 + \rho, \omega) - \bar{J}_2(1, \omega)) S(u, \rho; \omega)
$$
$$
+ H_1(0) \bar{J}_2(1, \omega) \int_0^\infty \frac{du}{u} \int_0^1 \frac{d\rho}{\rho} S(u, \rho; \omega), \quad (A3)
$$

where the $1/\delta$ divergence resides in the last term. We can now combine the two endpoint-divergent terms as

$$
\bar{J}_2(1, \omega) H_1(0) \left(\int_0^1 \frac{du}{u} \int_0^\infty \frac{d\rho}{\rho} + \int_0^\infty \frac{du}{u} \int_0^1 \frac{d\rho}{\rho} \right) S(u, \rho; \omega)
$$
$$
= \bar{J}_2(1, \omega) H_1(0) \left(\int_0^1 \frac{du}{u} \int_0^1 \frac{d\rho}{\rho} - \int_1^\infty \frac{du}{u} \int_1^\infty \frac{d\rho}{\rho} \right)
$$
$$
\times S(u, \rho; \omega)|_{\lambda^2 \to 0} \quad (A4)
$$

where we have used that in case of analytic regulators the scaleless double integral

$$
\int_0^\infty \frac{du}{u} \int_0^\infty \frac{d\rho}{\rho} S(u, \rho; \omega) = 0,
$$

vanishes. The indicated limit $\lambda^2 \to 0$ is understood to be performed after the convolutions, keeping the logarithmically enhanced terms. Notice that in the second term in brackets on the right-hand side of Eq. (A4) we can drop the analytic regulator and directly set $\lambda^2 \to 0$ in the soft function [in fact, for the leading expression $S^{(1)}(u, \rho; \omega)$, the $\mathcal{O}(\lambda^2)$ terms only contribute at $\mathcal{O}(\epsilon)$]. This term is thus insensitive to the long-distance dynamics of the muon and thus can be combined with the first term in the factorization theorem. Collecting all terms then leads to Eq. (56) in the main text.

It is instructive to consider the leading-order expressions for the individual contributions in the endpoint-subtracted factorization theorem (56). For the first line, we obtain

$$
\int_0^\infty \frac{du}{u} \left[H_1^{(0)}(u) \bar{J}_1^{(1)}(u;\omega)\theta(1-u) - H_1^{(0)}(0)\bar{J}_2^{(0)}(1,\omega)\theta(u-1) \int_1^\infty \frac{d\rho}{\rho} S^{(1)}(u\rho;\omega) \right]_{\lambda^2 \to 0}
$$
$$
= \left(\frac{\mu^2 e^{\gamma_E}}{2E\omega} \right)^\epsilon \int_0^\infty \frac{du}{u^{1+\epsilon}} \left[-\Gamma(\epsilon)(1-u)^{1-\epsilon} H_1^{(0)}(u)\theta(1-u) - H_1^{(0)}(0)\frac{\theta(u-1)}{\Gamma(1-\epsilon)} \int_1^\infty \frac{d\rho}{\rho^{1+\epsilon}} \right]
$$
$$
= \left(\frac{\mu^2}{2E\omega} \right)^\epsilon \int_0^1 du \left[\left(\delta(u) - \left[\frac{1-u}{u} \right]_+ \right) \frac{1}{\epsilon} + 2\delta(u) + \left[\frac{(1-u)\ln[u(1-u)]}{u} \right]_+ \right] H_1^{(0)}(u)
$$
$$
\equiv \int_0^1 du\, \bar{J}_1^{\mathrm{eff}(1)}(u) H_1^{(0)}(u). \tag{A5}
$$

We observe that the $1/\epsilon^2$ term that originally appeared in the anti-hard-collinear region from the endpoint divergence at $u \to 0$ is now canceled by the subtraction, and the remaining contributions can be obtained from an endpoint-finite convolution with an effective anti-hard-collinear function, which is distribution valued and reproduces the single-logarithmic term.

Similarly, for the second line of the endpoint-subtracted factorization theorem we find at leading order

$$
\bar{J}_2^{(0)}(1,\omega) \int_0^1 \frac{du}{u} [H_1^{(0)}(u)\bar{C}^{(1)}(u) - H_1^{(0)}(0)[[C^{(1)}(u)]]]
$$
$$
= \Gamma(\epsilon) \left(\frac{\mu^2 e^{\gamma_E}}{m^2} \right)^\epsilon \int_0^1 \frac{du}{u} [H_1^{(0)}(u)(1-u)^{1-2\epsilon} - H_1^{(0)}(0)]
$$
$$
= \left(\frac{\mu^2}{m^2} \right)^\epsilon \int_0^1 du \left[\left(-\delta(u) + \left[\frac{1-u}{u} \right]_+ \right) \frac{1}{\epsilon} \right.
$$
$$
\left. - \left(2 - \frac{\pi^2}{3} \right)\delta(u) - \left[\frac{2(1-u)\ln(1-u)}{u} \right]_+ \right] H_1^{(0)}(u)
$$
$$
\equiv \bar{J}_2^{(0)}(1,\omega) \int_0^1 du\, \bar{C}^{\mathrm{eff}(1)}(u) H_1^{(0)}(u), \tag{A6}
$$

which again only contains the single-logarithmic term. The associated $1/\epsilon$ divergence cancels with the one from the first line, see Eq. (A5), on the integrand level, with an

effective anticollinear function which is again distribution valued.

For the third line in the factorization theorem, we find

$$
H_1^{(0)}(0) \int_0^\infty \frac{d\rho}{\rho} [\bar{J}_2^{(0)}(1+\rho,\omega) - \theta(1-\rho)\bar{J}_2^{(0)}(1,\omega)]
$$
$$
\times \int_0^\infty \frac{du}{u} S^{(1)}(u\rho;\omega)
$$
$$
= \left(\frac{\mu^2 e^{\gamma_E}}{2E\omega} \right)^\epsilon \int_0^\infty \frac{d\rho}{\rho} \left[\frac{1}{1+\rho} - \theta(1-\rho) \right] \int_{\lambda^2/\rho}^\infty \frac{du}{u} \frac{(u\rho - \lambda^2)^{-\epsilon}}{\Gamma(1-\epsilon)}
$$
$$
= \Gamma(\epsilon) \left(\frac{\mu^2 e^{\gamma_E}}{m^2} \right)^\epsilon \int_0^\infty \frac{d\rho}{\rho} \left[\frac{1}{1+\rho} - \theta(1-\rho) \right] = 0, \tag{A7}
$$

and therefore the soft region does not contribute at leading order after subtraction.

Finally, as already stated in Eq. (44), the fourth line of the subtracted factorization theorem reproduces the anti-soft-collinear region with cutoffs,

$$
\bar{J}_2^{(0)}(1,\omega) H_1^{(0)}(0) \int_0^1 \frac{du}{u} \int_0^1 \frac{d\rho}{\rho} S^{(1)}(u\rho;\omega) \bigg|_{\lambda^2 \to 0} = \frac{1}{2}\ln^2\lambda^2.
$$

[1] R. Aaij *et al.* (LHCb Collaboration), First Evidence for the Decay $B_s^0 \to \mu^+\mu^-$, Phys. Rev. Lett. **110**, 021801 (2013).

[2] R. Aaij *et al.* (LHCb Collaboration), Measurement of the $B_s^0 \to \mu^+\mu^-$ Branching Fraction and Search for $B^0 \to \mu^+\mu^-$ Decays at the LHCb Experiment, Phys. Rev. Lett. **111**, 101805 (2013).

[3] S. Chatrchyan *et al.* (CMS Collaboration), Measurement of the $B_s^0 \to \mu^+\mu^-$ Branching Fraction and Search for $B^0 \to \mu^+\mu^-$ with the CMS Experiment, Phys. Rev. Lett. **111**, 101804 (2013).

[4] V. Khachatryan *et al.* (CMS, LHCb Collaborations), Observation of the rare $B_s^0 \to \mu^+\mu^-$ decay from the combined analysis of CMS and LHCb data, Nature (London) **522**, 68 (2015).

[5] M. Aaboud *et al.* (ATLAS Collaboration), Study of the rare decays of B_s^0 and B^0 into muon pairs from data collected during the LHC Run 1 with the ATLAS detector, Eur. Phys. J. C **76**, 513 (2016).

[6] R. Aaij *et al.* (LHCb Collaboration), Measurement of the $B_s^0 \to \mu^+\mu^-$ Branching Fraction and Effective Lifetime and

Search for $B^0 \to \mu^+\mu^-$ Decays, Phys. Rev. Lett. **118,** 191801 (2017).

[7] M. Aaboud *et al.* (ATLAS Collaboration), Study of the rare decays of B_s^0 and B^0 mesons into muon pairs using data collected during 2015 and 2016 with the ATLAS detector, J. High Energy Phys. 04 (2019) 098.

[8] A. M. Sirunyan *et al.* (CMS Collaboration), Measurement of properties of $B_s^0 \to \mu^+\mu^-$ decays and search for $B^0 \to \mu^+\mu^-$ with the CMS experiment, J. High Energy Phys. 04 (2020) 188.

[9] CMS Collaboration, LHCb Collaboration, and ATLAS Collaboration, Combination of the ATLAS, CMS and LHCb results on the $B^0_{(s)} \to \mu^+\mu^-$ decays, Technical Report No. CMS-PAS-BPH-20-003, LHCb-CONF-2020-002, AT-LAS-CONF-2020-049, CERN, Geneva, 2020.

[10] R. Aaij *et al.* (LHCb Collaboration), Analysis of Neutral *B*-Meson Decays into Two Muons, Phys. Rev. Lett. **128,** 041801 (2022).

[11] CMS Collaboration, Measurement of $B_s^0 \to \mu^+\mu^-$ decay properties and search for the $B^0 \to \mu\mu$ decay in proton-proton collisions at $\sqrt{s} = 13$ TeV, Technical Report No. CMS-PAS-BPH-21-006, CERN, Geneva, 2022.

[12] R. Aaij *et al.* (LHCb Collaboration), Measurement of the $B_s^0 \to \mu^+\mu^-$ decay properties and search for the $B^0 \to \mu^+\mu^-$ and $B_s^0 \to \mu^+\mu^-\gamma$ decays, Phys. Rev. D **105,** 012010 (2022).

[13] K. De Bruyn, R. Fleischer, R. Knegjens, P. Koppenburg, M. Merk, A. Pellegrino, and N. Tuning, Probing New Physics via the $B_s^0 \to \mu^+\mu^-$ Effective Lifetime, Phys. Rev. Lett. **109,** 041801 (2012).

[14] A. J. Buras, J. Girrbach, D. Guadagnoli, and G. Isidori, On the standard model prediction for $\mathcal{B}(B_{s,d} \to \mu^+\mu^-)$, Eur. Phys. J. C **72,** 2172 (2012).

[15] A. J. Buras, R. Fleischer, J. Girrbach, and R. Knegjens, Probing new physics with the $B_s \to \mu^+\mu^-$ time-dependent rate, J. High Energy Phys. 07 (2013) 077.

[16] C. Bobeth, M. Gorbahn, T. Hermann, M. Misiak, E. Stamou, and M. Steinhauser, $B_{s,d} \to l^+l^-$ in the Standard Model with Reduced Theoretical Uncertainty, Phys. Rev. Lett. **112,** 101801 (2014).

[17] R. Aaij *et al.* (LHCb Collaboration), Implications of LHCb measurements and future prospects, Eur. Phys. J. C **73,** 2373 (2013).

[18] W. Altmannshofer *et al.* (Belle-II Collaboration), The Belle II physics book, Prog. Theor. Exp. Phys. **2019,** 123C01 (2019); **2020,** 029201(E) (2020).

[19] M. Beneke, C. Bobeth, and R. Szafron, Enhanced Electromagnetic Correction to the Rare *B*-Meson Decay $B_{s,d} \to \mu^+\mu^-$, Phys. Rev. Lett. **120,** 011801 (2018).

[20] M. Beneke, C. Bobeth, and R. Szafron, Power-enhanced leading-logarithmic QED corrections to $B_q \to \mu^+\mu^-$, J. High Energy Phys. 10 (2019) 232.

[21] M. Beneke, P. Böer, J.-N. Toelstede, and K. K. Vos, QED factorization of non-leptonic *B* decays, J. High Energy Phys. 11 (2020) 081.

[22] M. Beneke, P. Böer, G. Finauri, and K. K. Vos, QED factorization of two-body non-leptonic and semi-leptonic *B* to charm decays, J. High Energy Phys. 10 (2021) 223.

[23] M. Beneke, P. Böer, J.-N. Toelstede, and K. K. Vos, Light-cone distribution amplitudes of light mesons with QED effects, J. High Energy Phys. 11 (2021) 059.

[24] M. Beneke, P. Böer, J.-N. Toelstede, and K. K. Vos, Light-cone distribution amplitudes of heavy mesons with QED effects, J. High Energy Phys. 08 (2022) 020.

[25] On the other hand, it has been shown in Ref. [20] that QCD/QED factorization theorems for the contributions of the semileptonic operators $\mathcal{O}_9$ and $\mathcal{O}_{10}$ can be obtained in the framework of soft-collinear effective theory without complications from endpoint divergences.

[26] M. Beneke and M. Neubert, QCD factorization for $B \to PP$ and $B \to PV$ decays, Nucl. Phys. **B675,** 333 (2003).

[27] Recent attempts to understand QCD factorization in $B_c \to \eta_c$ transitions in Ref. [28] indicate that a consistent treatment of endpoint divergences in exclusive charmless *B*-meson decays is more subtle than anticipated in Ref. [29].

[28] P. Böer, QCD factorisation in exclusive semileptonic B decays new applications and resummation of rapidity logarithms, Ph.D. thesis, Siegen University, 2018.

[29] C.-D. Lü, Y.-L. Shen, C. Wang, and Y.-M. Wang, Enhanced next-to-leading-order corrections to weak annihilation *B*-meson decays, arXiv:2202.08073.

[30] Z. L. Liu and M. Neubert, Factorization at subleading power and endpoint-divergent convolutions in $h \to \gamma\gamma$ decay, J. High Energy Phys. 04 (2020) 033.

[31] Z. L. Liu, B. Mecaj, M. Neubert, and X. Wang, Factorization at subleading power and endpoint divergences in $h \to \gamma\gamma$ decay. Part II. Renormalization and scale evolution, J. High Energy Phys. 01 (2021) 077.

[32] M. Beneke, M. Garny, S. Jaskiewicz, J. Strohm, R. Szafron, L. Vernazza, and J. Wang, Next-to-leading power endpoint factorization and resummation for off-diagonal "gluon" thrust, J. High Energy Phys. 07 (2022) 144.

[33] G. Bell, P. Böer, and T. Feldmann, Muon-electron backward scattering: A prime example for endpoint singularities in SCET, J. High Energy Phys. 09 (2022) 183.

[34] M. Beneke and V. A. Smirnov, Asymptotic expansion of Feynman integrals near threshold, Nucl. Phys. **B522,** 321 (1998).

[35] V. A. Smirnov and E. R. Rakhmetov, The Strategy of regions for asymptotic expansion of two loop vertex Feynman diagrams, Theor. Math. Phys. **120,** 870 (1999).

[36] T. Liu and A. Penin, High-energy limit of mass-suppressed amplitudes in gauge theories, J. High Energy Phys. 11 (2018) 158.

[37] K. G. Chetyrkin, M. Misiak, and M. Munz, Weak radiative B meson decay beyond leading logarithms, Phys. Lett. B **400,** 206 (1997); **425,** 414(E) (1998).

[38] T. Becher and M. Neubert, Drell-Yan production at small q_T, transverse parton distributions and the collinear anomaly, Eur. Phys. J. C **71,** 1665 (2011).

[39] T. Becher, G. Bell, and M. Neubert, Factorization and resummation for jet broadening, Phys. Lett. B **704,** 276 (2011).

[40] G. Bell, T. Feldmann, Y.-M. Wang, and M. W. Y. Yip, Light-cone distribution amplitudes for heavy-quark hadrons, J. High Energy Phys. 11 (2013) 191.

[41] M. I. Kotsky and O. I. Yakovlev, On the resummation of double logarithms in the process $H \to \gamma\gamma$, Phys. Lett. B **418,** 335 (1998).

[42] C. W. Bauer, S. Fleming, D. Pirjol, and I. W. Stewart, An effective field theory for collinear and soft gluons: Heavy to light decays, Phys. Rev. D **63,** 114020 (2001).

[43] We remark in passing that a very simple approximation for the net RG factor can be obtained by expanding in the coefficient b_0 of the QCD beta function. Considering, in addition, the natural relation between the individual matching scales, $\mu_0 \mu_h \equiv \mu_{hc}^2$, we obtain

$$
\begin{aligned}
H_1(0;\mu) &\bar{\mathcal{J}}_2(1,\omega',\mu) e^{V(\mu,\mu_0)} \left(\frac{\mu_0 e^{2\gamma_E}}{\omega'}\right)^{-g(\mu,\mu_0)} \Bigg|_{\mu_{hc}^2=\mu_0\mu_h} \\
&\simeq \exp\Bigg[-\frac{\alpha_s(\mu_{hc})C_F}{4\pi}\ln^2\frac{\mu_0}{\mu_h} + \frac{\alpha_s(\mu^*)C_F}{\pi}\ln\frac{\mu_0}{\mu_{hc}}\ln\frac{\mu_0 e^{2\gamma_E}}{\omega'} \\
&\quad + \mathcal{O}(b_0^2)\Bigg],
\end{aligned}
$$

where the scale $\mu_* = \sqrt{\mu_0\mu_{hc}}$ is determined by requiring that the $\mathcal{O}(b_0)$ corrections to the above approximation are

zero. The renormalization scale for the value of α_s that is relevant for the ω'-dependent RG effects is therefore given by the geometric mean of the hard-collinear and soft scale.

[44] T. Feldmann, P. Lüghausen, and D. van Dyk, Systematic parametrization of the leading B-meson light-cone distribution amplitude, J. High Energy Phys. 10 (2022) 162.

[45] In Ref. [20] the RG factor for $\lambda_{B_s}(\mu)$ is only considered in fixed-order approximation, without resumming logarithms $\ln\frac{\mu_{hc}}{\mu_0}$. Also note that the auxiliary parameter ω_0 is identified with λ_{B_s} in [20].

[46] D. Binosi and L. Theussl, JaxoDraw: A graphical user interface for drawing Feynman diagrams, Comput. Phys. Commun. **161,** 76 (2004).

[47] The separation of the ρ integration at $\rho = 1$ is convenient, but one could also cut the integral at $\rho = \rho_0 \sim \mathcal{O}(1)$ to obtain a more general formula.